

# Metal cation-exchanged montmorillonite catalyzed protection of aromatic aldehydes with Ac<sub>2</sub>O

L'uboš Jankovič and Peter Komadel\*

*Institute of Inorganic Chemistry, Slovak Academy of Sciences, 845 36 Bratislava, Slovakia*

Received 17 January 2003; revised 5 March 2003

## Abstract

The protection of aromatic aldehydes with acetic anhydride was investigated in the presence of 26 metal cation-exchanged montmorillonites (M<sup>n+</sup>-MMT) and commercial acid-activated K10 and KSF montmorillonites (Südchemie Moosburg, Germany). The acid sites of all catalysts were investigated by infrared spectroscopy and thermal analysis using pyridine as a molecular probe. The yield of reaction is roughly related to the strength of acid sites and depends also on the substitution on the benzene ring of the aldehydes. The order of activity of selected cation-exchanged forms was Al > K10 ~ KSF > Zn > Na which correlates well with the polarizing power of these cations and resulting acidity. Al<sup>3+</sup>-MMT is revealed to be an effective catalyst for protection of aromatic aldehydes with Ac<sub>2</sub>O and produces almost solely 1,1-diacetates. Relatively high yield of products observed for “moderately acid” cations, such as Zn<sup>2+</sup>, can be explained by the fact that protection of aldehydes requires medium-strength acid sites.

© 2003 Elsevier Inc. All rights reserved.

**Keywords:** Clay; Montmorillonite; Exchange; Acidity; Protection; Aldehyde; Acetic anhydride; 1,1-Diacetate

## 1. Introduction

Selective organic transformation in the presence of various solid catalysts including metal cation-exchanged clay minerals is of current interest in making the synthetic processes comfortable and benign to the Earth [1]. The ability of variously exchanged montmorillonites to catalyze a range of organic reactions of synthetic and industrial significance remains attractive for chemists [2–4]. The catalytic activity could be explained in terms of either Lewis or Brønsted acid centers contributing to the reaction mechanism [5]. Clay catalysts have been shown to contain both Brønsted and Lewis acid sites, with the Brønsted sites mainly associated with the interlamellar region and the Lewis sites mainly associated with edge sites. The acidity of smectites is influenced by the quantity of water between the layers [6,7].

In the interlayer space basic and acidic adsorption sites are present [8]. The oxygens of the O planes and exchangeable metal cations are electron pair donors and acceptors, or Lewis bases and acids, respectively. Since the interlayer

space contains water under ambient conditions, the contribution of the Lewis bases and acids to the overall surface acidity of the interlayer is only secondary. However, Lewis base and acid properties are revealed when the adsorption of an organic compound is accompanied by expulsion of the interlayer water.

Water molecules in the hydration spheres of exchangeable cations are proton donors (Brønsted acids). Hydration water dissociates under the polarizing effect of the metallic cation as follows:



where  $x$  is the number of water molecules that directly coordinate the metal cation  $M$  and  $m+$  is the charge on the cation. A similar cation polarizing effect occurs in aqueous salt solutions, but it is much more significant in the interlayer space of clay minerals. The reason for this enhancement is the dielectric constant of interlayer water, which is less than that of ordinary water; consequently, protons in the interlayer are more mobile than in bulk water [9–11]. The degree of dissociation of water is 10<sup>7</sup> times higher in the interlayer space than in liquid water [12].

Most of the methods utilized for the determination of the acidity of acid-treated clays are time consuming [13].

\* Corresponding author.

*E-mail addresses:* [uachljan@savba.sk](mailto:uachljan@savba.sk) (L. Jankovič),  
[uachkomp@savba.sk](mailto:uachkomp@savba.sk) (P. Komadel).

Several studies have shown that thermogravimetric analysis of the desorption of bases, such as butylamine, cyclohexylamine, and pyridine, can be used to evaluate rapidly the amount and type of acid sites in clay minerals [13–15]. The technique of temperature-programmed desorption (TPD) has been used to considerable advantage for elucidation of the number and type of adsorption sites on a wide range of solid surfaces which exhibit catalytic properties. However, as with many physical techniques, the results from the TPD technique cannot be interpreted in isolation and corroborative evidence is generally sought from infrared (IR) spectra.

The first step in the activation procedure, which is required for both natural and synthetic clay minerals, is to convert the mineral into the desired ion form. In the case of metal ions, this can be achieved relatively easily by ion exchange using a concentrated solution of a suitable salt, followed by repeated washings to remove the excess salt. As an alternative, one can use ion-exchange resins in suitable ion forms.

There is still a great demand for heterogeneous catalysis under mild conditions and in environmentally friendly processes. Montmorillonites, a class of inexpensive and non-corrosive solid acids, have been used as efficient catalysts for a variety of organic reactions. The reactions catalyzed by montmorillonites are usually carried out under mild conditions with high yields and high selectivities and the workup of these reactions is very simple; only filtration to remove the catalyst and evaporation of the solvent are required. Montmorillonite catalysts are easily recovered and reused [16,17].

Some frequently used organic reactants containing reactive groups, such as aldehydes and ketones, require protection of these groups to avoid undesirable side reactions. Protection of aldehyde with acetic anhydride in the presence of montmorillonite catalyst is a suitable reaction for testing the catalytic activity of modified smectites [18]. An earlier assay showed that heated  $\text{NH}_4^+$ -MMT catalyzed protection of 3,4,5-trimethoxybenzaldehyde [19]. The aim of this work was to prepare various homoionic montmorillonites from a  $\text{Ca}^{2+}$ -form by ion exchange and to test catalytic activity of these materials for the conversion of benzaldehyde, 3,4,5-trimethoxybenzaldehyde and 4-nitrobenzaldehyde in acetic anhydride into diacetate.

## 2. Experimental

Montmorillonite separated from bentonite from the deposit Ivančice (Czech Republic) was used for the experiments. Bentonite was ground in an agate mortar and a  $< 2\text{-}\mu\text{m}$  fraction was separated by sedimentation in order to remove most of the impurities. In the course of this process, the sample was repeatedly saturated with a calcium chloride solution to obtain a homoionic form of montmorillonite. The metal cation-exchanged forms ( $\text{M}^n$ -MMT) were prepared from the  $\text{Ca}^{2+}$  form via multiple overnight saturation with  $1\text{ mol dm}^{-3}$   $\text{M}^n\text{Cl}_n$  or  $\text{M}^n(\text{NO}_3)_n$  solutions. Excess salt

was removed afterward by washing with distilled water until a negative test for chlorides with silver nitrate solution or for nitrates with sodium salicylate solution/ $\text{H}_2\text{SO}_4$ . The metal cation-exchanged montmorillonites were dried at  $60^\circ\text{C}$  and ground to pass a 0.2-mm sieve.

Commercially available acid montmorillonite-based catalysts K10 and KSF were obtained from the manufacturer (Südchemie Moosburg, Germany). Solvents and chemicals were obtained from Merck (reagent grade) and were used as supplied.

All catalytic tests were performed in small glass flasks using 10 mg smectite immersed in 10 ml of a 0.02 M solution of aldehyde in acetic anhydride. The reaction mixture was kept under stirring at  $20^\circ\text{C}$  for 1 h. This reaction time was chosen on the basis of preliminary results obtained with K10 and was suitable for all the different reactions and catalysts studied. Ten microliters portions of the liquid phase were removed from the flasks with a syringe, diluted to 1 ml with acetonitrile, and analyzed using HPLC chromatography. Blank experiments (without a catalyst) were performed simultaneously. Three parallel catalytic experiments were carried out for each catalyst.

The samples for both thermal analysis and IR spectroscopy were air-dried prior to exposure to reagent grade pyridine vapor at room temperature for periods of 5 days. Samples ( $\sim 20\text{ mg}$ ) were transferred directly from the desiccator with pyridine vapor into the equipments.

## 3. Analytical methods

### 3.1. Fourier transform infrared (FTIR) spectroscopy

The DRIFTS (diffuse reflectance IR) spectra were obtained using a diffuse-reflectance accessory “Collector” from Spectra-Tech at room temperature without a dilution in KBr on a FTIR spectrometer Nicolet Magna 750 equipped with a DTGS detector. Samples were quickly poured loosely into a sample cup of  $\sim 1\text{ mm}$  depth and 3 mm diameter. For each sample, 128 scans were recorded in the  $4000\text{--}400\text{ cm}^{-1}$  spectral range with a resolution of  $4\text{ cm}^{-1}$ .

### 3.2. Thermal analysis

The TG analyses (DTG curves are shown) were conducted from ambient temperature up to  $700^\circ\text{C}$  using a T.A.I. SDT 2960 instrument ( $\sim 20\text{-mg}$  sample mass,  $10^\circ\text{C min}^{-1}$  in flowing air).

### 3.3. HPLC chromatography

Samples were analyzed using a Hewlett Packard HP-1090M HPLC apparatus with a Hypersil column (BDS  $5\text{ }\mu\text{m}/200 \times 2.1\text{ mm}$ ) and a mobile phase consisting of a mixture of water and acetonitrile (1:1). Detection was performed with a diode array detector at 210 nm and the products were

identified by the retention times of reference substances. Differences in the determined concentrations of the reaction products in three parallel runs were always within  $\pm 2\%$  from the average reported. The yield was determined as the percentage of the reactant converted to the reaction product.

#### 4. Results and discussion

The infrared absorption bands in the  $1400\text{--}1700\text{ cm}^{-1}$  region for pyridine adsorbed on silica-alumina and aluminosilicates have been used to study their acidity since the 1960 [20–22]; however, the nature of acid sites on MMT has not been completely elucidated yet. It is known that spectra of MMT before pyridine adsorption contain in this region only one band near  $1630\text{ cm}^{-1}$  due to the bending OH vibrations of water molecules. Analysis of the bands reported in the IR spectra after the adsorption of pyridine on montmorillonite shows that there are four types of adsorption sites (Fig. 1).

The Brønsted sites (B) show bands near  $1490$ ,  $1540$ , and  $1635\text{ cm}^{-1}$  [6,14]. The  $1540\text{ cm}^{-1}$  band is typical of this site; the corresponding species is the pyridinium ion ( $\text{PyH}^+$ ). It is assumed that tricoordinated aluminum atoms with an electron-free orbit constitute Lewis acid centers (L). Pyridine coordinated to the Lewis sites absorbs near  $1455$ ,  $1490$ , and  $1610\text{--}1625\text{ cm}^{-1}$ ; the  $1455\text{ cm}^{-1}$  band is typical of these sites [23]. The third type of site, corresponding to hydrogen-bonded pyridine (H) on the clay solid [20,24], has vibrations near  $1440$  and  $1590\text{ cm}^{-1}$ . These bands are probably due to a strong interaction between the cation and the pyridine molecule, by attraction of the cation into the electrostatic field [25]. Liengme and Hall [26] suggested another type of Lewis site and attributed the  $1445\text{ cm}^{-1}$  band to the (skeletal) ring-stretching vibration of pyridine coordinately bonded to the residual  $\text{Na}^+$  cations on dehydroxylated Y-type zeolites. This pyridine-cationized mordenite band was strong enough to be present even after evacuation at  $450^\circ\text{C}$ . Finally, the vibration near  $1575\text{ cm}^{-1}$  is con-

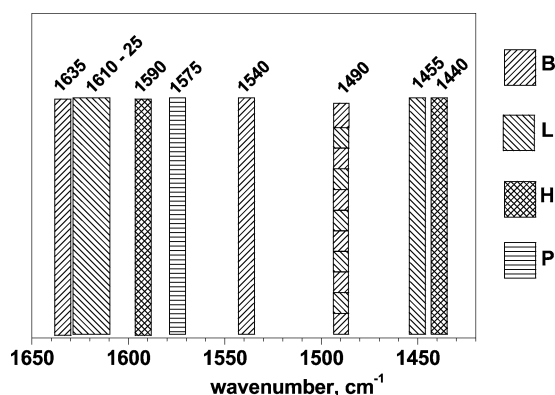


Fig. 1. Bands in the IR spectra of acid solids with adsorbed pyridine in the  $1420\text{--}1650\text{ cm}^{-1}$  region. Pyridine adsorbed on B, Brønsted sites; L, Lewis sites; H, hydrogen-bonded, and P, physisorbed pyridine.

nected with very weak adsorption corresponding either to simple nonspecific physical adsorption (P in Fig. 1) or to an extremely weak specific coordination of pyridine in MMT, in strength similar to interactions of pyridine molecules in liquid phase [20,24].

Fig. 2 presents representative IR spectra of the selected air-dried metal-exchanged montmorillonites, taken after their exposure to pyridine. The samples exhibited absorption bands which, following Breen et al. [14], were assigned to physisorbed pyridine ( $\sim 1577$  and  $\sim 1440\text{ cm}^{-1}$ ), hydrogen-bonded pyridine ( $\sim 1440$  and  $1590\text{ cm}^{-1}$ ), Lewis-bound pyridine ( $\sim 1450$ ,  $1490$ ,  $1590$ , and  $1620\text{ cm}^{-1}$ ), pyridine coordinated through its aromatic  $\pi$ -electrons ( $1607\text{ cm}^{-1}$ ), and the pyridinium cation ( $1540$  and  $1640\text{ cm}^{-1}$ ).

The samples with alkali and alkali earths cations contained no Brønsted acid sites, only coordinately bound pyridine (the bands near  $1440$ ,  $1490$ ,  $1590$ , and  $1625\text{ cm}^{-1}$  in the spectrum of  $\text{Na}^+$ -MMT, Fig. 2). The bands near  $1440$  and  $1590\text{ cm}^{-1}$  indicated hydrogen-bonded pyridine. The bands near  $1490$  and  $1625\text{ cm}^{-1}$  could be ascribed to pyridine adsorption on Lewis acid sites, but absence of the  $1450\text{ cm}^{-1}$  band makes this assignment improbable. The broad band near  $1625\text{ cm}^{-1}$  was of low intensity, which could indicate some amount of strong and/or Lewis acid centers or rather vibrations of remaining water molecules. This is more probable because no band was observed due to pyridinium ion near  $1540\text{ cm}^{-1}$ , which would be indicative of Brønsted acidity. Assignment of this band to vibrations of water is supported by its easy removal upon heating [14]. Finally, the band near  $1575\text{ cm}^{-1}$  and partially the band near  $1440\text{ cm}^{-1}$  (more exactly, a component of this complex band) can be

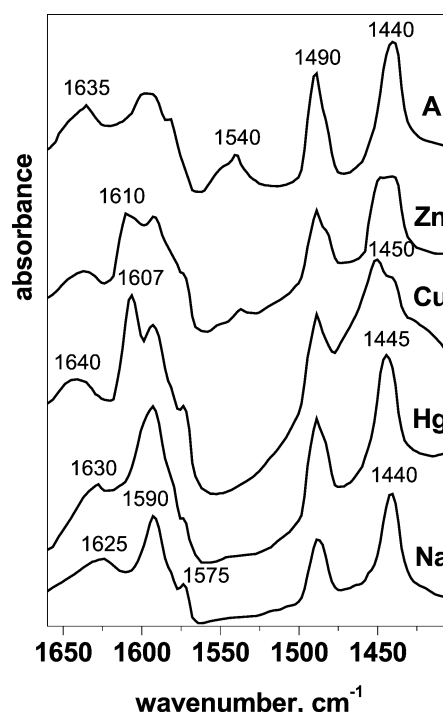


Fig. 2. DRIFT spectra of pyridine-saturated catalysts.

attributed to physical adsorption of pyridine in MMT with alkali and alkali earths cations.

The spectra of  $\text{Hg}^{2+}$ -,  $\text{Cu}^{2+}$ -, and  $\text{Zn}^{2+}$ -MMTs containing predominantly Lewis sites are shown in Fig. 2. Intensities of the bands due to sorbed pyridine on typical Lewis acid sites were moderate to high, e.g., the  $1445\text{ cm}^{-1}$  band in the spectrum of  $\text{Hg}^{2+}$ -MMT. The band near  $1490\text{ cm}^{-1}$  could be attributed to sorption of pyridine on both Brønsted and/or Lewis sites while the band near  $1590\text{ cm}^{-1}$  was assigned to hydrogen-bonded pyridine. Both these bands are rather broad, suggesting a relatively wide range of strengths of these acid sites. Intensities of these bands are higher than in the spectrum of  $\text{Na}^+$ -MMT (Fig. 2). Bands near  $1570$  and  $1630\text{ cm}^{-1}$  represented the physisorbed and Lewis pyridine and/or remaining water molecules, respectively, as described above.

Two bands at  $1450$  and  $1573\text{ cm}^{-1}$  observed in the spectrum of  $\text{Cu}^{2+}$ -MMT (Fig. 2) were due to interaction of pyridine with Lewis centers and physisorption. No band was observed near  $1540\text{ cm}^{-1}$ ; therefore, the band near  $1490\text{ cm}^{-1}$  is considered to show only Lewis sites. The very broad band near  $1640\text{ cm}^{-1}$  includes vibration of water and interaction of pyridine with the Lewis sites. Pyridine bands at  $1592$  and  $1607\text{ cm}^{-1}$  indicated two types of pyridine, i.e., pyridine hydrogen-bonded to water and pyridine directly coordinated to the copper ion, respectively [27]. The spectrum of this deep blue sample contained absorption bands near  $1440$  and  $1590\text{ cm}^{-1}$ , indicating the presence of hydrogen-bonded pyridine. The intense  $1607\text{ cm}^{-1}$  band occurred only in the spectrum of  $\text{Cu}^{2+}$ -MMT and was ascribed to pyridine coordinated to copper through its aromatic  $\pi$ -electrons rather than through the nitrogen atom. A change in color of  $\text{Cu}^{2+}$ -MMT upon adsorption of pyridine from the liquid phase was ascribed to a pyridine free radical [28]. The formation and further reactions of free radicals may be catalyzed by copper ions and these radicals could contribute to both the intense color and unusual absorption of IR radiation by the copper-pyridine complexes in montmorillonite.

The spectrum of  $\text{Zn}^{2+}$ -MMT (Fig. 2), as well as the spectra of  $\text{Co}^{2+}$ -,  $\text{Ni}^{2+}$ -,  $\text{Cd}^{2+}$ -,  $\text{Sn}^{2+}$ -,  $\text{Mn}^{2+}$ -,  $\text{Bi}^{3+}$ -, and  $\text{Sb}^{3+}$ -MMTs (not shown), exhibited similar bands as observed for the spectrum of  $\text{Cu}^{2+}$ -MMT. The shift of the band near  $1445\text{ cm}^{-1}$  can be interpreted as evidence of Lewis acidity of these forms. It is easily observed in case of the  $\text{Zn}^{2+}$ -MMT, which contains broad bands created by overlap of the bands at  $1440$  and  $1450\text{ cm}^{-1}$ , assigned as hydrogen-bonded and Lewis acid site interaction of pyridine. In addition, the intensive band at  $1610\text{ cm}^{-1}$  suggested the presence of Lewis acid centers and the band near  $1540\text{ cm}^{-1}$  of low intensity signified the presence of relatively small amount of Brønsted acid sites.

The  $\text{Al}^{3+}$ -,  $\text{La}^{3+}$ -,  $\text{Fe}^{3+}$ -,  $\text{Ce}^{3+}$ -,  $\text{Cr}^{3+}$ -, and  $\text{Zr}^{4+}$ -exchanged forms, as well as K10 and KSF catalysts (only the spectrum of  $\text{Al}^{3+}$ -MMT is shown in Fig. 2), contained predominantly Brønsted acid sites [6,14,29] and the intensity of the band near  $1540\text{ cm}^{-1}$  was higher in comparison with

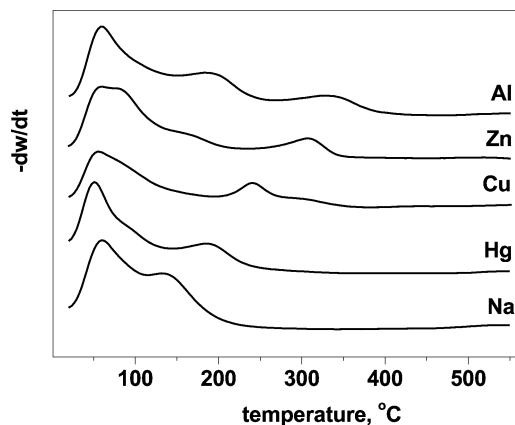


Fig. 3. Derivative thermograms for desorption of pyridine from  $\text{M}^{n+}$ -montmorillonites.

the other forms. Similarly as described above, the band at  $1490\text{ cm}^{-1}$  reflected the presence of both Lewis and Brønsted acid centers. The bands near  $1585$  and  $1595\text{ cm}^{-1}$  and that near  $1440\text{ cm}^{-1}$  corresponded to physisorbed and hydrogen-bonded pyridine of the catalysts, respectively. Intensities of all the bands except for that near  $1570\text{ cm}^{-1}$  were higher than in the spectra of the other forms described above, proving higher acidity of  $\text{M}^{3+}$ -MMTs. This was confirmed by the high intensities of the “typical” Brønsted band near  $1540\text{ cm}^{-1}$  in the spectra of  $\text{Al}^{3+}$ -,  $\text{La}^{3+}$ -,  $\text{Fe}^{3+}$ -,  $\text{Ce}^{3+}$ -,  $\text{Cr}^{3+}$ -, and  $\text{Zr}^{4+}$ -MMTs and by the absence of a diagnostic Lewis band near  $1455\text{ cm}^{-1}$ .

Desorption of pyridine from different sites upon heating provides additional information on adsorption sites on solid catalysts [14]. Fig. 3 shows how the derivative thermogravimetric profiles for several cation-exchanged montmorillonites saturated with pyridine vary with the nature of the exchangeable cation. The peak at  $50^\circ\text{C}$  occurred in all hydrated  $\text{M}^{n+}$ -MMT and may be attributed to dehydration. Besides it, the  $\text{Na}^+$ -MMT exhibited a maximum near  $130^\circ\text{C}$ , which can be ascribed to desorption of pyridine. No protonation of pyridine was observed for the alkali and alkaline-earth cation-exchanged forms, only the trace of  $\text{Na}^+$ -MMT is shown in Fig. 3. Only one desorption maximum from acid sites was observed near  $190^\circ\text{C}$  in the traces of  $\text{Hg}^{2+}$ - (Fig. 3) and  $\text{Pb}^{2+}$ -MMT (not shown), suggesting that these two forms contain only Lewis acid sites, i.e., sites of moderate acid strength. However, the IR spectra showed that some stronger acid sites could be present.  $\text{Cu}^{2+}$ -MMT had a desorption peak near  $240^\circ\text{C}$  (Fig. 3), which can be attributed to desorption from acid sites of moderate strength and/or to thermal decomposition of pyridinium copper complex formed after exposition of  $\text{Cu}^{2+}$ -MMT to pyridine vapor. Formation of such a complex is supported by IR spectroscopy results as well as by the change of sky-blue color to charming depth azurite after exposition to pyridine.

Desorption profiles for the  $\text{Zn}^{2+}$ -,  $\text{Co}^{2+}$ -,  $\text{Cd}^{2+}$ -,  $\text{Ni}^{2+}$ -,  $\text{Sn}^{2+}$ -,  $\text{Bi}^{3+}$ -,  $\text{Sb}^{3+}$ -, and  $\text{Zr}^{4+}$ -MMTs showed three desorption peaks (only the trace of  $\text{Zn}^{2+}$ -MMT is shown in

Table 1

Ionic potentials of selected ions and acidity values, obtained from pyridine desorption between 300 and 400 °C, of montmorillonite saturated with these cations

Cation $M^{n+}$	Ionic potential ( $e \text{ \AA}^{-1}$ )	Acidity of $M^{n+}$ -MMT ( $\text{mmol g}^{-1}$ )
$\text{Na}^+$	1.05	0.118
$\text{Hg}^{2+}$	1.82	0.169
$\text{Cu}^{2+}$	2.90	0.357
$\text{Zn}^{2+}$	2.69	0.536
$\text{Al}^{3+}$	6.00	0.699

Fig. 3). The components at 50 and 90 °C were attributed to desorption of water and pyridine, respectively [14], while that near 310 °C indicated the presence of protonated pyridine. The desorption profiles for K10, KSF, and the  $\text{Al}^{3+}$ -,  $\text{La}^{3+}$ -,  $\text{Ce}^{3+}$ -,  $\text{Fe}^{3+}$ -,  $\text{Cr}^{3+}$ -, and  $\text{Mn}^{2+}$ -MMTs were very similar; thus only the trace for  $\text{Al}^{3+}$ -MMT is displayed, showing three peaks at 50, 190, and 330 °C (Fig. 3). They were attributed to physisorbed, Lewis-bound and protonated pyridine, respectively. This is in accord with the interpretation of the corresponding peaks in the desorption profile for cyclohexylamine [13].

Table 1 shows ionic potentials of selected cations and acidity values, obtained from pyridine desorption between 300 and 400 °C, of the same forms of montmorillonite as shown in Figs. 2 and 3. Pyridine desorption in this temperature range is attributed to pyridine bound to strong acid sites, i.e., the sites of the highest catalytic potential. Generally, with increasing ionic potential (charge/radius ratio) of the cation the acidity of the montmorillonite form increased. An apparent exception is zinc, which is more acidic than would be expected from its ionic potential. Zinc chloride adsorbed on montmorillonite is catalytically very active [16].

As the clay acidity depends on the nature of the exchangeable cation, the catalytic activity of this series of cation-exchanged montmorillonites for protection of aromatic aldehydes with acetic anhydride was investigated [29]. The most probable reaction mechanism is that the aldehyde group is activated by the acid centers present on the catalyst, followed by a nucleophilic attack of the acetanhydride molecule (Scheme 1).

This reaction is considered to be a suitable alternative for preparation of 1,1-diacetates from aldehydes, with the advantage of selectivity, operational simplicity, high yields, short reaction times, and minimal environmental impact [18]. The advantages for the tests of catalysts include high stability of reaction products and their relatively easy and simple analysis, as well as sensitivity to the presence of



Table 2

Yields of reaction of R-benzaldehydes with  $\text{Ac}_2\text{O}$  catalyzed with  $M^{n+}$ -montmorillonites

$M^{n+}$	R		
	H	3,4,5-MeO	4-NO <sub>2</sub>
$\text{H}^+$ (K10)	80	62	90
$\text{H}^+$ (KSF)	81	63	92
$\text{Li}^+$	13	5	26
$\text{Na}^+$	16	3	27
$\text{K}^+$	17	4	26
$\text{Rb}^+$	14	6	25
$\text{Cs}^+$	15	4	28
$\text{Mg}^{2+}$	19	5	27
$\text{Ca}^{2+}$	16	4	28
$\text{Sr}^{2+}$	18	2	26
$\text{Ba}^{2+}$	14	3	29
$\text{Al}^{3+}$	83	60	95
$\text{Sn}^{2+}$	30	15	44
$\text{Pb}^{2+}$	33	11	42
$\text{Zr}^{4+}$	67	42	76
$\text{Cr}^{3+}$	77	52	84
$\text{Mn}^{2+}$	43	20	54
$\text{Fe}^{3+}$	80	57	89
$\text{Co}^{2+}$	45	23	56
$\text{Ni}^{2+}$	47	28	57
$\text{Cu}^{2+}$	41	19	53
$\text{Zn}^{2+}$	70	54	83
$\text{Cd}^{2+}$	41	24	52
$\text{Hg}^{2+}$	33	17	45
$\text{Ce}^{3+}$	77	54	85
$\text{Sb}^{3+}$	49	25	55
$\text{Bi}^{3+}$	45	21	53
$\text{La}^{3+}$	79	57	88

weak acid sites in the catalysts [30]. Therefore, it is a suitable reaction for testing catalytic activity of modified smectites. The results of catalytic tests are shown in Table 2.

It appeared that  $\text{La}^{3+}$ ,  $\text{Cr}^{3+}$ ,  $\text{Ce}^{3+}$ ,  $\text{Fe}^{3+}$ ,  $\text{Al}^{3+}$ ,  $\text{Zn}^{2+}$ ,  $\text{Zr}^{4+}$ , and  $\text{H}^+$  were the most efficient cations, while other exchanged montmorillonite gave moderate ( $\text{Co}^{2+}$ ,  $\text{Cd}^{2+}$ ,  $\text{Cu}^{2+}$ ,  $\text{Hg}^{2+}$ ,  $\text{Mn}^{2+}$ ,  $\text{Ni}^{2+}$ ,  $\text{Pb}^{2+}$ ,  $\text{Sn}^{2+}$ ,  $\text{Sb}^{3+}$ ,  $\text{Bi}^{3+}$ ) or low ( $\text{Li}^+$ ,  $\text{Na}^+$ ,  $\text{K}^+$ ,  $\text{Rb}^+$ ,  $\text{Cs}^+$ ,  $\text{Mg}^{2+}$ ,  $\text{Ca}^{2+}$ ,  $\text{Sr}^{2+}$ ,  $\text{Ba}^{2+}$ ) yields of the product. According to Adams [31], the  $M^{3+}$ -MMTs are expected to be more active than divalent (except  $\text{Zn}^{2+}$ ) or monovalent ion-exchanged minerals.  $\text{Zr}^{4+}$ -MMT was less active than  $\text{H}^+$ -MMTs in the acylation reaction, which can be explained by the fourfold lower amount of  $\text{Zr}^{4+}$  than  $\text{H}^+$  compensating negative charge of the layers and/or by  $\text{Zr}^{4+}$  hydrolysis to form polymeric type species. Noteworthy is that  $\text{Ce}^{3+}$ -faujasite was more active than  $\text{Ce}^{3+}$ -MMT under similar reaction conditions [32]. This suggests that the cation effect on the activity of a catalyst depends on the mineral framework and its negative charge, which is higher for zeolite than for montmorillonite. It is worth returning to the Brønsted acid-catalyzed protection of substituted aromatic aldehydes to examine the relationship between activity and Brønsted acid strength. This is not quite straightforward because pyridine desorption acidity measurements provide combined Brønsted and Lewis acidities. Nevertheless, the

infrared data in Fig. 2 show very clearly that the  $\text{Al}^{3+}$ -MMT has both the strongest and the most abundant acid sites, and this is almost certainly a reflection of the surface Brønsted acidity on this catalyst. The activity of the  $\text{Al}^{3+}$ -MMT in the acid-catalyzed reaction is the highest of the group. A reasonable correlation was found for the surface acidity and catalytic activity for other ion-exchanged MMTs. For all three aldehydes the  $\text{Al}^{3+}$  form was the most active catalyst. The highest Brønsted acidity of exchangeable  $\text{Al}^{3+}$  in  $\text{Al}^{3+}$ -MMT is generated when the ions are only partially hydrated, so that the ion's ability to polarize directly coordinated water molecules is maximized. The acid-treated catalysts K10 and KSF were highly active in the acid-catalyzed protection of aldehydes due to either the amount or the accessibility of the surface acid sites. The importance of active site accessibility in catalysts of this type was illustrated for Friedel–Craft reactions catalyzed by K10 and a series of pillared clays. The reaction was diffusion-controlled in the pillared clay catalysts and the superior activity of the K10 was due largely to its wider pores and more accessible acid sites [33]. Although the metal exchanged catalysts used here exhibit smaller pores than the pillared clays, it is likely that diffusion control is more important in these catalysts than in K10.

Catalytic activities of ion-exchanged clay minerals in both Brønsted and Lewis acid-catalyzed reactions reflect the surface acidities of the catalysts. The trend shown in Brønsted acidity is predictable, and can be explained in terms of the abilities of the exchangeable cations in the catalyst to polarize the coordinating water molecules and hence generate protons.  $\text{Ca}^{2+}$ -MMT and other forms with alkali and alkali earth cations gave very low yields and in a control experiment without any catalyst no reaction occurred. The catalysts in these forms show the lowest activity, confirming that the exchangeable cations are indeed the active sites. Experiment with initiating reaction by adding the aldehyde to premixed catalyst K10 plus anhydride showed no difference in the results of catalytic activity. The yields obtained with different catalysts and aldehydes show that the reaction yield depends on the reactivity of the aldehyde molecule, which is connected with the substituents, rather than on the basicity of the aldehyde, thus proving the mechanisms shown in Scheme 1.

Catalytic activity of the prepared materials was tested in the reaction of preparation of (R-phenyl)methylene diacetate from R-benzaldehyde ( $\text{R} = \text{H}, 4\text{-NO}_2, 3,4,5\text{-MeO}$ ). These liquid-phase reactions are relatively facile and simple, and only single quite stable products are formed. The reactants in these three reactions contain the same functional groups and so the factors associated with the active sites on the catalysts are likely to be similar. Neither reaction requires or produces water. Water could affect the strength of acid sites on clay surfaces and could hydrate Lewis acid centers converting them to Brønsted acid sites.

The effect of substitution of benzaldehydes on the catalyzed reaction involved electron donating or withdrawing forces of the substituting group. The nitro group, in contrast

to the methoxy group, has a strong electron-withdrawing effect and therefore the expected order of reactivity for substituted aldehydes was  $\text{NO}_2 > \text{H} > \text{MeO}$ . The results obtained evidently support this order, and average differences in the yield of reaction between experiments with various aldehydes was  $\sim 10\%$  for the unsubstituted and 4-nitrobenzaldehyde and about  $20\%$  for the 3,4,5-trimethoxy- and benzaldehyde. More reactive 4-nitrobenzaldehyde reacted faster than the other two and the lowest yields of the products were achieved with the least reactive 3,4,5-trimethoxybenzaldehyde. Concerning the role of the catalyst, it is well stated that reactions on montmorillonites generally involve previous adsorption and diffusion of reactant through the pores and interlayers. However, in the present liquid phase reaction, the acid sites on the external surface of the catalyst play a crucial role in the activation of reactant molecules particularly with large and bulky compounds such as 3,4,5-trimethoxybenzaldehyde and its 1,1-diacetate. In fact, under these conditions the interlayer spaces are completely filled with solvent, reactant, and product molecules and the curvature effects on the external surface of the clay catalyst are likely to promote reagent activation and process selectivity [30,33,34].

## 5. Conclusions

Catalytic activity of metal cation-exchanged montmorillonites was tested for the protection of three substituted aldehydes with acetic anhydride. Both the alkali and the alkaline earth cation-exchanged forms were of low catalytic activity due to their low surface acidity, which is documented by the IR spectra of adsorbed pyridine and DTG desorption traces. Many of exchanged forms with divalent cations of transition metals were of moderate catalytic activity, though not fully approaching the activity of the acid-activated montmorillonite catalysts K10 and KSF. Pyridine interaction experiments showed presence of both Lewis and Brønsted acid sites, but did not allow their exact quantification. The high activity of  $\text{Fe}^{3+}$ ,  $\text{Al}^{3+}$ ,  $\text{La}^{3+}$ ,  $\text{Cr}^{3+}$ ,  $\text{Zn}^{2+}$ , and  $\text{Ce}^{3+}$  forms is due to the formation of stronger acid sites resulting from the polarizing ability of these cations. The Brønsted acidity, giving rise to the catalytic activity of clay minerals, is derived from the polarization of solvent water molecules by the small, highly charged interlayer cations. Consequently, the high catalytic activity of  $\text{Al}^{3+}$ - compared to  $\text{Fe}^{3+}$ - and  $\text{Cr}^{3+}$ -exchanged montmorillonites has been attributed to the enhanced polarization of water molecules in the primary coordination sphere of the  $\text{Al}^{3+}$  cation.

## Acknowledgments

Financial support of VEGA, the Grant Agency of the Slovak Republic (Grant No. 2/7202/00) is acknowledged.

## References

- [1] M. Balogh, in: L.A. Paquette (Ed.), *Encyclopedia of Reagents for Organic Synthesis*, Vol. 2, Wiley, Chichester, 1995, p. 1356.
- [2] J.A. Ballantine, in: R. Setton (Ed.), *Chemical Reactions in Organic and Inorganic Constrained Systems*, Reidel, Holland, 1986, pp. 197–212.
- [3] M. Balogh, P. Laszlo, *Organic Chemistry Using Clays*, Springer, Berlin, 1993.
- [4] R.S. Varma, *Tetrahedron* 58 (2002) 1235.
- [5] J.M. Thomas, in: M.S. Whittingham, A.J. Jacobson (Eds.), *Intercalation Chemistry*, Academic Press, New York, 1982, pp. 56–97.
- [6] D.R. Brown, C.N. Rhodes, *Catal. Lett.* 45 (1997) 35.
- [7] H.H.P. Yiu, D.R. Brown, *Catal. Lett.* 56 (1998) 57.
- [8] S. Yariv, K.H. Michaelian, *Schriftenr. Angew. Geowiss.* 1 (1997) 180.
- [9] G. Sposito, R. Prost, *Chem. Rev.* 82 (1982) 553.
- [10] N.T. Skipper, A.K. Soper, J.D.C. McConnell, K. Refson, *Chem. Phys. Lett.* 166 (1990) 141.
- [11] C.H. Bridgeman, N.T. Skipper, *J. Phys.: Condens. Matter* 9 (1997) 4081.
- [12] R. Touillaux, P. Salvador, C. Vandermeersche, J.J. Fripiat, *Isr. J. Chem.* 6 (1968) 337.
- [13] J.A. Ballantine, P. Graham, I. Patel, J.H. Purnell, K.J. Williams, in: L.G. Schulz, H. van Olphen, F. Mumpton (Eds.), *Proc. Int. Clay Conf. Denver, 1985*, The Clay Minerals Society, Bloomington, 1987, p. 311.
- [14] C. Breen, A.T. Deane, J.J. Flynn, *Clay Miner.* 22 (1987) 169.
- [15] C. Breen, J. Forsyth, J. Yarwood, T. Hughes, *Phys. Chem. Chem. Phys.* 2 (2000) 3887.
- [16] D.R. Brown, *Geol. Carpathica, Ser. Clays* 45 (1994) 45.
- [17] P. Laszlo, *Preparative Chemistry Using Supported Reagents*, Academic Press, San Diego, 1987.
- [18] Z.H. Zhang, T.S. Li, C.G. Fu, *J. Chem. Res. (S)* (1997) 174.
- [19] L. Jankovič, P. Komadel, *Collect. Czech. Chem. Commun.* 65 (2000) 1527.
- [20] E.P. Parry, *J. Catal.* 2 (1963) 371.
- [21] J.W. Ward, *J. Colloid Interface Sci.* 28 (1968) 269.
- [22] H. Hatori, T. Shiba, *J. Catal.* 12 (1968) 111.
- [23] F. Kooli, W. Jones, *Clay Miner.* 32 (1997) 633.
- [24] C. Breen, *Clay Miner.* 26 (1991) 487.
- [25] J.W. Ward, *J. Catal.* 10 (1968) 34.
- [26] B.V. Liengme, W.K. Hall, *Trans. Faraday Soc.* 62 (1966) 3229.
- [27] V.C. Farmer, M.M. Mortland, *J. Chem. Soc.* (1966) 344.
- [28] R.M. Barrer, D.M. Macleod, *Trans. Faraday Soc.* 50 (1954) 980.
- [29] N.Y. Chen, W.E. Garwood, F.G. Dwyer, *Shape-Selective Catalysis in Industrial Applications*, Dekker, New York, 1989.
- [30] M.V. Joshi, C.S. Narasimhan, D. Mukesh, *Zeolites* 15 (1995) 597.
- [31] J.M. Adams, T.V. Clapp, D.E. Clement, *Clay Miner.* 18 (1983) 411.
- [32] B. Chiche, A. Finiels, C. Gauthier, P. Geneste, *J. Mol. Catal.* 42 (1987) 229.
- [33] R. Mokaya, W. Jones, *J. Catal.* 153 (1995) 76.
- [34] R. Ballini, G. Bosica, B. Frullanti, R. Maggi, G. Sartori, F. Schroer, *Tetrahedron Lett.* 39 (1998) 1615.